Optica Applicata, Vol. XLIV, No. 3, 2014
DOI: 10.5277/oa140302

Fluctuations in settling velocity of red blood cell aggregates

ADAM KEMPCZYŃSKI, MACIEJ BOSEK, BRONISŁAW GRZEGORZEWSKI*

Biophysics Department, Collegium Medicum in Bydgoszcz, Nicolaus Copernicus University, ul. Jagiellońska 13, 85-067 Bydgoszcz, Poland

*Corresponding author: grzego@cm.umk.pl

Sedimentation of red blood cell aggregates was experimentally investigated by optical imaging. Suspensions of red blood cell at low hematocrit were obtained from blood of healthy donors. The velocity of three-dimensional red blood cell aggregates was measured using particle image velocimetry. The magnitude and spatial correlation functions of the velocity fluctuations of the settling aggregates were determined. It is shown that the fluctuations in the settling velocity exhibit characteristic correlations in the form of swirls. The formation of 3-D red blood cell aggregates leads to a large initial swirl. The growth of the aggregates and their sedimentation diminishes the swirls size.

Keywords: particle image velocimetry, red blood cell aggregation, sedimentation, velocity fluctuations.

1. Introduction

Sedimentation of a suspension of particles is an important issue in many areas of science, technology and medicine. Ever since the pioneering work of BATCHELOR [1] in the early 1970s, many efforts were made to understand the sedimentation of non-Brownian monodisperse spherical particles. The mean settling velocity gives some insight into how sedimentation takes place, while fluctuations of velocity, caused by long-range hydrodynamic interactions, considerably provide more information about the process. Theoretical considerations predict a divergence of the magnitude of the fluctuations with system size [2] while most experiments do not confirm this divergence [3, 4]. The velocity fluctuations reveal long-range correlations, in the form of swirls, and scaling of the swirl size has been found [4]. The numerical simulations of sedimentation of non-isotropic and deformable particles exhibit similarities to the sedimentation process of spherical particles, however, they are much more non-stationary [5]. Moreover the description of the processes observed for sedimenting spherical particles for higher volume fraction rather cannot be simple extrapolation of that for lower volume fraction [6, 7]. Although recent numerous studies have brought a wealth of information on the settling dynamics of particles, the authors agree that an understanding of the sedimentation process is far from complete.

An investigation of the red blood cell (RBC) sedimentation process is significant from a medical point of view. RBCs are flexible, biconcave discs that tend to form aggregates in the presence of proteins or polymers [8]. Suspended RBCs form linear or branched aggregates called *rouleaux*, which later coalesce into three-dimensional (3-D) RBC aggregates [9]. These large aggregates sediment and form a deposit at the bottom of a container [9, 10]. RBC sedimentation has been studied theoretically since the turn of the 1980s [11] but the proposed models were insufficient in explaining the process. In investigations of RBC aggregation and sedimentation, difficulties still arise in identifying how the objects form and sediment [12, 13]. The formation of rouleaux has been studied both experimentally [14–17] and theoretically [18]. To investigate the size of the particles, the light scattering study of RBC suspensions has been performed [19–21]. Recently, new theoretical techniques are developed for the analysis of optical fields scattered by particles with possible application in biomedicine [22–24]. Formation and sedimentation of 3-D RBC aggregates are much less recognized. However, the velocity of 3-D aggregates was frequently studied with the use of the image analysis, where Fourier method [25], Hough method [25, 26] as well as particle image velocimetry [27] were applied. The differences between the suspension of monodisperse rigid spheres and blood suggest that the sedimentation process in these systems may be significantly different. Thus, 3-D RBC aggregate dynamics remains one of the most important problems to be resolved in order to provide more insight into RBC sedimentation.

In this paper, the sedimentation of 3-D RBC aggregates was investigated. The velocity of the settling 3-D RBC aggregates was measured using particle image velocimetry. The aim of the paper is to describe the long-range correlations in the fluctuations of the aggregates velocity.

2. Material and method

The blood of healthy donors was examined in this study. The RBCs were extracted from the blood, washed in phosphate saline buffer and resuspended in autologous plasma at hematocrit 0.03, 0.05 and 0.07. A rectangular glass-walled container 30 mm wide, 1 mm deep and 30 mm high was used to perform the sedimentation experiment. The container was filled by injection of RBCs suspended in plasma. Measurements were performed at room temperature 22 ± 1°C. A sequence of images of the suspension was obtained using an optical system shown in Fig. 1. The light from an illumination system passed through the container with the blood sample and next was registered by an imaging system. The imaging system with a CCD camera (1280×960 pixels) was focused on a plane near the wall of the container. It sampled a cross-section of the container sized 9×12 mm^2, located 8 mm above the bottom of the container. Images were taken every second. This period is approximately equal to the minimal ratio of the radius of the observed objects, estimated using the correlation function of the intensity in the image plane to their sedimentation velocity.

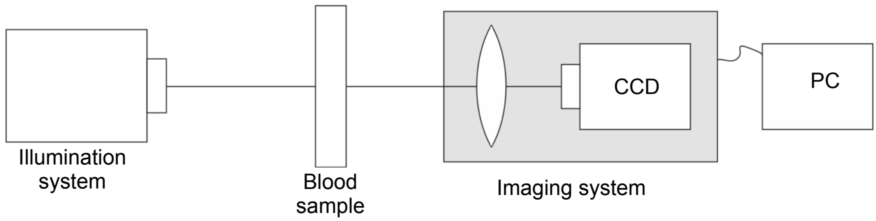

Fig. 1. Experimental setup.

The Reynolds number $Re = 2aV_{sed}\rho/\eta$ and the Péclet number $Pe = \pi a^2 V_{sed}\eta/kT$ of the sedimenting particles were estimated, where sedimentation velocity V_{sed} and aggregate radius a are taken from the experiment, $\rho = 1030$ kg/m^3 is the density of the plasma, $\eta = 1.6\times10^{-3}$ Pa·s is the viscosity of the plasma, T is the temperature and k is the Boltzmann constant. These numbers for RBC aggregates change in time during the process. The Reynolds number was very low, $Re < 4.1\times10^{-3}$. The Péclet number after the initial 300 s was attaining very high values, $Pe > 1.2\times10^4$. Thus, the motion of the RBC aggregates was practically unaffected by thermal fluctuations and inertial effects.

RBC aggregate velocities **V** were obtained using particle image velocimetry (PIV). LabView software was applied to process the data. Two-dimensional RBC aggregate velocity-vector fields were received. Each velocity vector was determined by a cross-correlation of the interrogation regions from successive pairs of images with the accuracy of 2 μm/s. The interrogation region, in the first step, was 64×64 pixels (0.64×0.64 mm^2) and next, to increase accuracy, it was decreased to 32×32 pixels (0.32×0.32 mm^2). The velocity fluctuation fields were determined from the velocity fields using the formula $\delta\mathbf{V} = \mathbf{V} - \langle\mathbf{V}\rangle$.

3. Results and discussion

The RBC aggregates occurring at characteristic times during the process at hematocrit 0.05 are displayed in Fig. 2. The experimental technique does not enable the precise identification of individual objects that appear up to about 300 s. During this initial

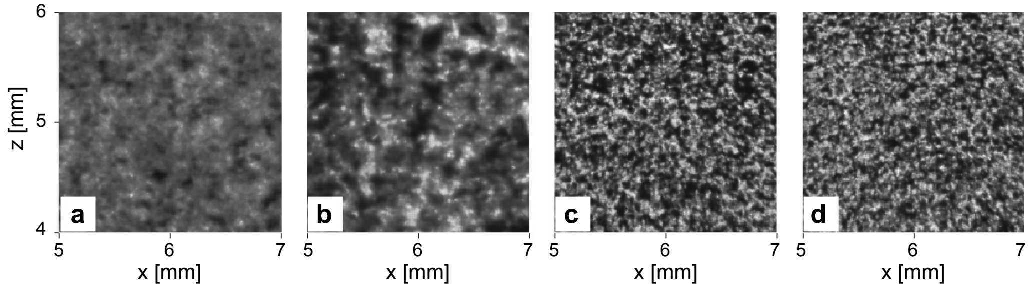

Fig. 2. Images of the suspension of RBC aggregates obtained at 300 s (**a**), 600 s (**b**), 1700 s (**c**) and 2000 s (**d**).

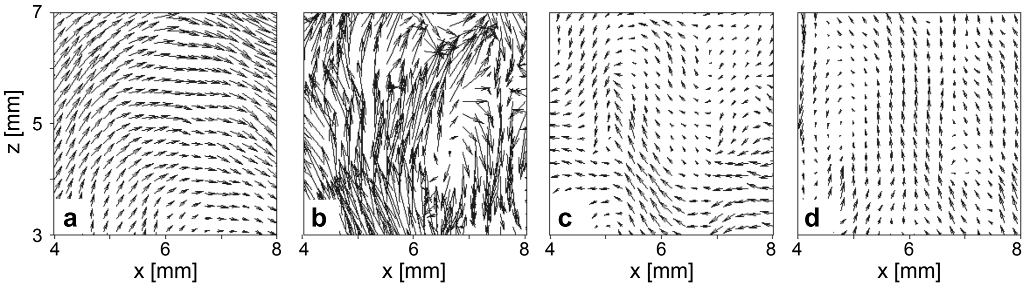

Fig. 3. Velocity fluctuation fields obtained for the suspension of RBC aggregates at 300 s (**a**), 600 s (**b**), 1700 s (**c**) and 2000 s (**d**). The respective vectors of the velocity fluctuations $\delta\mathbf{V}$ are at a fixed magnification of the vector scale.

phase, the RBC rouleaux formation mainly occurred. At 300 s just formed 3-D RBC aggregates appeared in the suspension. At 600 s the formation of the aggregates is completed and the largest aggregates can be observed. Later due to a stratification, the fraction of small 3-D RBC aggregates dominates in the area of observation. The velocity fluctuations of these aggregates were estimated and the velocity fluctuation fields appearing at these times are shown in Fig. 3. The velocity fluctuation fields reveal regions of correlated movement of the aggregates in the form of swirls. Figure 3 shows that the formation of 3-D RBC aggregates is associated with creation of a large initial swirl. The growth of the aggregates causes creation of smaller swirls. To quantify the size of the swirls, the autocorrelation functions of the velocity fluctuations [4] were analyzed. This function was determined in a vertical direction for the horizontal velocity fluctuations, $C_x(z) = \langle \delta V_x(0)\delta V_x(z)\rangle$, and in a horizontal direction for the vertical velocity fluctuations $C_z(x) = \langle \delta V_z(0)\delta V_z(x)\rangle$. It should be noted that in the above formulas the angled brackets represent an average from the data given by a single velocity field as the data are available only from the RBC sedimentation experiment. Figure 4 shows the velocity correlations in both directions. The position of the first

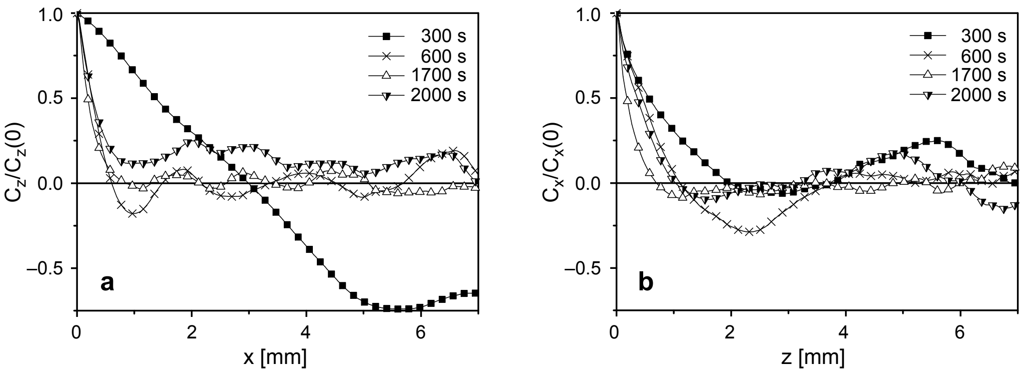

Fig. 4. Normalized autocorrelation functions determined in the vertical direction for the horizontal velocity fluctuations $C_z(x)/C_z(0)$ (**a**), and in the horizontal direction for the vertical velocity fluctuations $C_x(z)/C_x(0)$ (**b**) obtained at 300 s, 600 s, 1700 s and 2000 s.

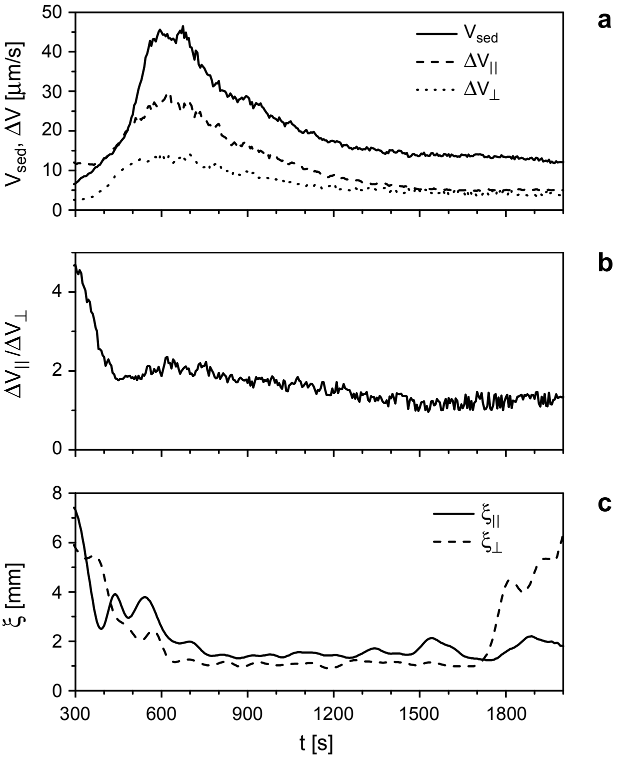

Fig. 5. Time evolution of the parameters of the RBC sedimentation process at hematocrit 0.05: sedimentation velocity V_{sed}, vertical $\Delta V_{||}$ and horizontal $\Delta V_{\perp}$ velocity fluctuations (**a**), the ratio between vertical and horizontal velocity fluctuations $\Delta V_{||}/\Delta V_{\perp}$ (**b**) and the vertical $\xi_{||}^{x}$ and horizontal $\xi_{\perp}^{z}$ correlation length of, respectively, horizontal and vertical velocity fluctuations (**c**).

minimum of these functions in a vertical and horizontal direction defines the correlation length, $\xi_{||}^{x}$ and $\xi_{\perp}^{z}$, representing, respectively, the vertical and horizontal size of the swirls.

Figure 5 summarizes the results obtained for the RBC sedimentation process. These results reveal the non-stationary behavior of this process. The sedimentation velocity $V_{\text{sed}} = \langle V_z \rangle$, as well as the vertical and horizontal velocity fluctuations, $\Delta V_{||} = \langle \delta V_z^2 \rangle^{1/2}$ and $\Delta V_{\perp} = \langle \delta V_x^2 \rangle^{1/2}$, respectively, first increased, at about 600 s reached a maximum value and finally decreased (Fig. 5**a**). As it is shown in Fig. 5**b** at the maximum of the aggregate velocity, the ratio between vertical and horizontal velocity fluctuations was close to 2 and next it began to decrease. Figure 5**c** shows that at 300 s formed aggregates initially created a large swirl. The growth of the aggregates at time interval from 300 to 600 s caused decay of the initial transient swirl. After 600 s, in the investigated region, smaller aggregates appeared. Figure 5**c** shows that the smaller 3-D RBC aggregates created smaller swirls, which after stabilizing become vertically elongated. After about 1700 s the swirls again increased. In this final phase of the process, the investigated region was depleted of large aggregates and it was occu-

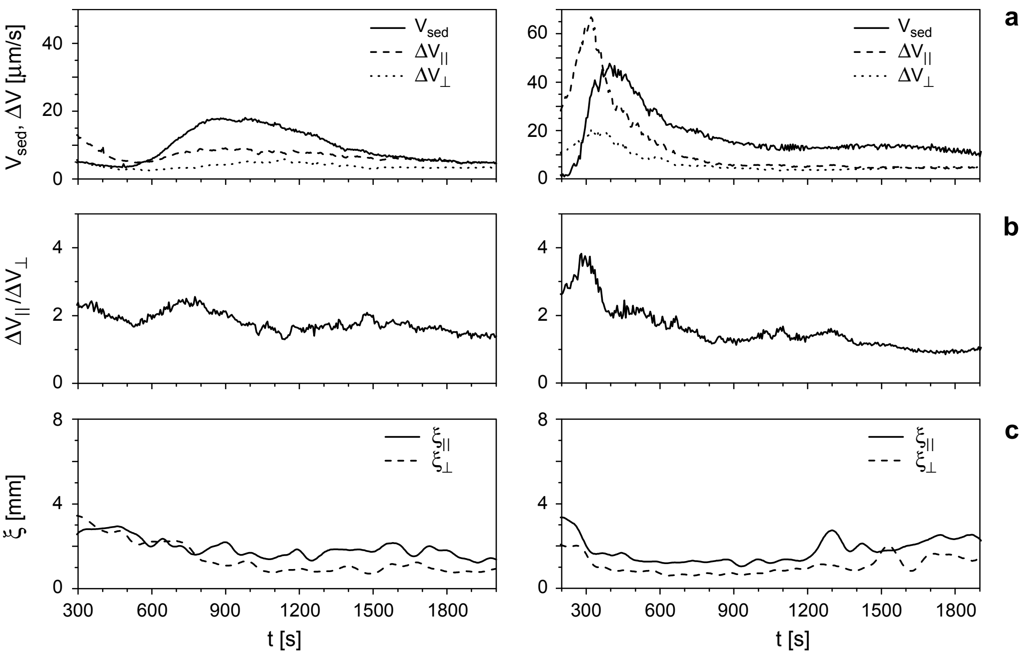

Fig. 6. Time evolution of the parameters of the RBC sedimentation process at hematocrit 0.03 (left column) and 0.07 (right column): sedimentation velocity V_{sed}, vertical $\Delta V_{||}$ and horizontal $\Delta V_{\perp}$ velocity fluctuations (**a**), the ratio between vertical and horizontal velocity fluctuations $\Delta V_{||}/\Delta V_{\perp}$ (**b**) and the vertical $\xi_{||}^{x}$ and horizontal $\xi_{\perp}^{z}$ correlation length of, respectively, horizontal and vertical velocity fluctuations (**c**).

pied by small slowly sedimenting aggregates, which can be observed in Fig. 2**d**. In Figure 6 the same evolutions at hematocrit 0.03 and 0.07 were shown. It is seen that in spite of the complexity of the process, the main features of these evolutions can be observed for the investigated samples.

The sedimentation of the 3-D RBC aggregates has some common features with the sedimentation of monodisperse rigid spheres. For the monodisperse spheres scaling laws for the size of the swirls $\xi = 15a\varphi^{-1/3}$ and for the velocity fluctuations $\Delta V_{||}/V_{sed} = 2\varphi^{1/3}$ and $\Delta V_{\perp}/V_{sed} = \varphi^{1/3}$ have been found [4]. Furthermore, in the suspension of rigid spheres cessation of mixing causes creation of a large initial swirl which relatively quickly decays to reach the size predicted by the scaling laws [28]. In this paper, it was shown that the formation of the 3-D RBC aggregates gives a comparable effect, *i.e.*, in both cases an initial large swirl was observed. Next, when smaller swirls appear, the ratio between vertical and horizontal velocity fluctuations of the largest RBC aggregates were about 2, as was found by SEGRÈ for monodisperse spheres before the front arrives [4]. The most important common feature of the processes was the long--range correlations of the velocity fluctuations in the form of swirls. However, in general, the results presented in this paper show that the settling dynamics of 3-D RBC aggregates exhibits much higher complexity than that of spherical monodisperse particles. A departure from the results for monodisperse spheres, similar to the case of the RBC aggregates, was observed by SAINTILLAN *et al.* [5] in the study of the sedimentation of spheroids and deformable particles. Both for RBC aggregates as well as spheroids and deformable particles, the sedimentation velocity and the velocity fluctuations exhibited non-stationary behavior. The growth of 3-D RBC aggregates stimulates an increase in sedimentation velocity and velocity fluctuations. For non-isotropic prolate particles as well as for deformable particles, these parameters increased with time as a result of the forming of clusters. This increase was also due to the vertical orienting of non-isotropic particles and deforming of deformable particles. After attaining the maximum, the sedimentation velocity and velocity fluctuations for these particles decreased with time, which was caused by considerable stratification in the suspension. A decrease of the RBC aggregate size exhibits high polydispersity of the aggregates and the stratification in their suspension. So, similarly as to the case of spheroids and deformable particles, stratification in the suspension of RBC aggregates decreased the sedimentation velocity and velocity fluctuations. The mean size of the swirls created by the spheres and spheroids was stable up to the arrival of the sedimentation front. For RBC aggregates, this stabilization appeared despite a lack of a clear sedimentation front. In the RBC suspension, the stabilization of the swirls size was observed as long as there were enough sedimenting RBC aggregates. Finally, for spheroids as well as for RBC aggregates, the swirls, at the final stage of their evolution, again increased, whereas for the spheres they vanished.

4. Conclusion

In this study, a new approach to the problem of RBC aggregate sedimentation was proposed. It allowed the revealing of long-range correlations of 3-D RBC aggregate velocity fluctuations in the form of swirls. Although we have found common features of the 3-D RBC aggregate sedimentation and sedimentation of monodisperse spheres, differences between the processes are significant. The growth of 3-D RBC aggregates stimulates similar behavior of the systems as the clustering effect. The results show new mechanisms of the RBC sedimentation process. In this way, these effects should be taken into account in the formulation of RBC sedimentation theory.

Acknowledgements – This work was supported by the UMK grant.

References

[1] BATCHELOR G.K., *Sedimentation in a dilute dispersion of spheres*, Journal of Fluid Mechanics **52**(2), 1972, pp. 245–268.

[2] CAFLISCH R.E., LUKE J.H.C., *Variance in the sedimentation speed of a suspension*, Physics of Fluids **28**(3), 1985, pp. 759–760.

[3] NICOLAI H., GUAZZELLI E., *Effect of the vessel size on the hydrodynamic diffusion of sedimenting spheres*, Physics of Fluids **7**(1), 1995, pp. 3–5.
[4] SEGRÈ P.N., HERBOLZHEIMER E., CHAIKIN P.M., *Long-range correlations in sedimentation*, Physical Review Letters **79**(13), 1997, pp. 2574–2577.
[5] SAINTILLAN D., SHAQFEH E.S.G., DARVE E., *The growth of concentration fluctuations in dilute dispersions of orientable and deformable particles under sedimentation*, Journal of Fluid Mechanics **553**, 2006, pp. 347–388.
[6] SEGRÈ P.N., LIU F., UMBANHOWAR P., WEITZ D.A., *An effective gravitational temperature for sedimentation*, Nature **409**(6820), 2001, pp. 594–597.
[7] SNABRE P., POULIGNY B., METAYER C., NADAL F., *Size segregation and particle velocity fluctuations in settling concentrated suspensions*, Rheologica Acta **48**(8), 2009, pp. 855–870.
[8] ARMSTRONG J.K., WENBY R.B., MEISELMAN H.J., FISHER T.C., *The hydrodynamic radii of macromolecules and their effect on red blood cell aggregation*, Biophysical Journal **87**(6), 2004, pp. 4259–4270.
[9] FABRY T.L., *Mechanism of erythrocyte aggregation and sedimentation*, Blood **70**(5), 1987, pp. 1572–1576.
[10] MUTRYNOWSKA J., GRZEGORZEWSKI B., *Optical analysis of red blood cell sediment formation*, Biorheology **44**(4), 2007, pp. 285–297.
[11] REUBEN A.J., SHANNON A.G., *Some problems in the mathematical modelling of erythrocyte sedimentation*, Mathematical Medicine and Biology **7**(3), 1990, pp. 145–156.
[12] PRIBUSH A., MEYERSTEIN N., *Methodological aspects of erythrocyte aggregation*, Recent Patents on Anti-Cancer Drug Discovery **2**(3), 2007, pp. 240–245.
[13] PRIBUSH A., MEYERSTEIN D., MEYERSTEIN N., *The mechanism of erythrocyte sedimentation. Part 2: The global collapse of settling erythrocyte network*, Colloids and Surfaces B: Biointerfaces **75**(1), 2010, pp. 224–229.
[14] PONDER E., *On sedimentation and rouleaux formation–II*, Experimental Physiology **16**(2), 1926, pp. 173–194.
[15] KERNICK D., JAY A.W.L., ROWLANDS S., SKIBO L., *Experiments on rouleau formation*, Canadian Journal of Physiology and Pharmacology **51**(9), 1973, pp. 690–699.
[16] SHIGA T., IMAIZUMI K., HARADA N., SEKIYA M., *Kinetics of rouleaux formation using TV image analyzer. I. Human erythrocytes*, American Journal of Physiology – Heart and Circulatory Physiology **245**(2), 1983 pp. H252–H258.
[17] BARSHTEIN G., WAJNBLUM D., YEDGAR S., *Kinetics of linear rouleaux formation studied by visual monitoring of red cell dynamic organization*, Biophysical Journal **78**(5), 2000, pp. 2470–2474.
[18] SAMSEL R.W., PERELSON A.S., *Kinetics of rouleau formation. I. A mass action approach with geometric features*, Biophysical Journal **37**(2), 1982, pp. 493–514.
[19] POP C.V.L., NEAMTU S., *Aggregation of red blood cells in suspension: study by light-scattering technique at small angle*, Journal of Biomedical Optics **13**(4), 2008, article 041308.
[20] TSINOPOULOS S.V., SELLOUNTOS E.J., POLYZOS D., *Light scattering by aggregated red blood cells*, Applied Optics **41**(7), 2002, pp. 1408–1417.
[21] SHVARTSMAN L.D., FINE I., *Optical transmission of blood: effect of erythrocyte aggregation*, IEEE Transactions on Biomedical Engineering **50**(8), 2003, pp. 1026–1033.
[22] BEKSHAEV A.YA., ANGELSKY O.V., HANSON S.G., ZENKOVA C.YU., *Scattering of inhomogeneous circularly polarized optical field and mechanical manifestation of the internal energy flows*, Physical Review A **86**, 2012, article 023847.
[23] SHEPPARD C.J.R., *Fractal model of light scattering in biological tissue and cells*, Optics Letters **32**(2), 2007, pp. 142–144.
[24] MIN XU, *Electric field Monte Carlo simulation of polarized light propagation in turbid media*, Optics Express **12**(26), 2004, pp. 6530–6539.

[25] Kempczyński A., Bosek M., Grzegorzewski B., *Comparison of Hough and Fourier transform approach in the study of kinetics of red blood cell aggregates*, Proceedings of SPIE **7141**, 2008, article 714118.

[26] Kempczyński A., Grzegorzewski B., *Estimation of red blood cell aggregate velocity during sedimentation using the Hough transform*, Optics Communications **281**(21), 2008, pp. 5487–5491.

[27] Kaliviotis E., Dusting J., Balabani S., *Spatial variation of blood viscosity: modelling using shear fields measured by a μPIV based technique*, Medical Engineering and Physics **33**(7), 2011, pp. 824–831.

[28] Bergougnoux L., Ghicini S., Guazzelli E., Hinch J., *Spreading fronts and fluctuations in sedimentation*, Physics of Fluids **15**(7), 2003, pp. 1875–1887.

Received May 21, 2014
in revised form July 11, 2014